Eur. Phys. J. B (2018) 91: 29
https://doi.org/10.1140/epjb/e2017-80530-8

THE EUROPEAN PHYSICAL JOURNAL B

Regular Article

Dependence of structure factor and correlation energy on the width of electron wires

Vinod Ashokan[1], Renu Bala[2], Klaus Morawetz[3,4,5,a], and Kare Narain Pathak[1]

[1] Centre for Advanced Study in Physics, Panjab University, Chandigarh 160014, India
[2] Department of Physics, MCM DAV College for Women, Chandigarh 160036, India
[3] Muenster University of Applied Physics, Stegerwaldstrasse 39, 48565 Steinfurt, Germany
[4] International Institute of Physics – UFRN, Campus Universitário Lagoa nova, 59078-970 Natal, Brazil
[5] Max-Planck-Institute for the Physics of Complex Systems, 01187 Dresden, Germany

Received 16 September 2017 / Received in final form 14 November 2017
Published online 7 February 2018

Abstract. The structure factor and correlation energy of a quantum wire of thickness $b \ll a_B$ are studied in random phase approximation (RPA) and for the less investigated region $r_s < 1$. Using the single-loop approximation, analytical expressions of the structure factor are obtained. The exact expressions for the exchange energy are also derived for a cylindrical and harmonic wire. The correlation energy in RPA is found to be represented by $\epsilon_c(b, r_s) = \frac{\alpha(r_s)}{b} + \beta(r_s)\ln(b) + \eta(r_s)$, for small b and high densities. For a pragmatic width of the wire, the correlation energy is in agreement with the quantum Monte Carlo simulation data.

1 Introduction

The motion of electrons confined in one spatial dimension gives rise to a variety of interesting phenomena with anomalous properties [1]. Recently quasi one-dimensional systems are experimentally realized in carbon nanotubes [2–5], semiconducting nanowires [6,7] and cold atomic gases [8–10], edge states in quantum hall liquid [11–13] and conducting molecules [14]. The electrons in one dimension do not obey the conventional Fermi-liquid theory, hence the prospect to observe non-Fermi-liquid features has given a large impetus to both theoretical and experimental research. An appropriate description of the one-dimensional (1D) homogeneous electron gas is provided by the low-energy theory based on an exactly solvable Tomonaga-Luttinger model [15–17]. The random phase approximation (RPA) is the correct theory for a homogeneous electron gas in the high-density limit i.e. at large electron densities $n = 1/(2r_s a_B)$, with a_B being the effective Bohr radius and r_s being the coupling parameter.

We model the interactions by a smoothed long-range Coulomb potential $v(x) \propto (x^2 + b^2)^{-1/2}$, where b is a parameter related to the width of the wire. We also use a harmonic confinement potential. The true long-range character of the Coulomb potential has been studied by Schulz [18] and Fogler [19,20] using a different approximation than RPA in certain domains of (b, r_s). In fact, a considerable amount of theoretical and numerical work has been done in this domain [21–34] using RPA, its generalized version and other methods, but still there is a need to understand the accurate parametrization of correlation energy for thin wires in the high-density limit. Therefore the calculation of the ground-state energy for thin wires in the high-density limit for realistic long-range Coulomb interactions is still an open problem for the 1D homogeneous electron gas.

Recently Lee and Drummond [35] have studied the ground state properties of the 1D electron liquid for an infinitely thin wire, and the harmonic wire using a quantum Monte Carlo (QMC) method, and provided a benchmark of the total energy data for a limited range of r_s. Furthermore, the harmonic wire with transverse confinement has been investigated with a lattice regularized diffusion Monte Carlo (LRDMC) technique by Casula et al. [36], and by others [37–39].

Loos [40] has considered the high-density correlation energy for the 1D homogeneous electron gas using the conventional perturbation theory by taking the smoothed Coulomb potential described above in the limit $b \to 0$ (infinitely thin wire). At $b = 0$ they have reported a correlation energy of -27.4 mHartree per electron at $r_s \to 0$. In their calculations the divergences in the integral for small b cancels out exactly. Although there is no direct comparison possible between results of Loos [40] and de Oliveira and Verri [32] with the RPA result due to use of different method of calculations, however, we mention that in RPA the correlation energy diverges for $b \to 0$ and $r_s \to 0$. The exchange energy has been found to be independent of b (leaving the logarithmic thickness $\mathcal{L}$ which may be cancelled with the uniform charge background). Further,

[a] e-mail: morawetz@fh-muenster.de

the agreement between the RPA result with QMC for the structure factor [41] ensures that the RPA should recover the normal Coulomb operator.

The purpose of the present paper is to study electron correlation effects in the interacting electron fluid described by RPA at high densities. The dependence of the structure factor and correlation energy on the wire-width is analyzed in the domain of $r_s < 1$ and $b \ll a_B$. In this respect it is noted that RPA is a good approximation in the high density limit $r_s \to 0$. We derive analytical expressions for the static structure factor in the high-density limit. The exact analytical expression for the exchange energy is also obtained for cylindrical and harmonic potentials. It is found that on the basis of theoretical deduction and a logical assumption, the correlation energy can be represented by the formula $\epsilon_c(b, r_s) = \frac{\alpha(r_s)}{b} + \beta(r_s)\ \ln(b) + \eta(r_s)$.

The paper is organized as follows. In Section 2, we calculate the static structure factor within RPA and using the first-order approximation. In Section 3, the RPA ground-state energy formula is given. Subsection 3.1 provides the exact analytical result of exchange energy for cylindrical and harmonic potentials for finite b and r_s. The result for small-b limit is also given there. Subsection 3.2 describes the correlation energy partially by an analytical formula and partially through numerical calculation. Then the final result of the correlation energy and its parametrization is presented. In Section 4 the results are discussed.

2 Structure factor

The structure factor $S(q)$ is now calculated within the RPA and its first-order version, where it is possible to obtain the result analytically. The RPA density response function $\chi(q, \omega)$ is given by [42],

$$\chi(q, \omega) = \frac{\chi_0(q, \omega)}{1 - V(q)\ \chi_0(q, \omega)}, \tag{1}$$

where $V(q)$ is the Fourier transform of the inter-electronic interaction potential. For harmonically trapped electron wires, and for cylindrical wires [26], it is given respectively by $V(q) = \frac{e^2}{4\pi\epsilon_0}\ E_1(b^2q^2)\ e^{b^2q^2}$ and $V(q) = 2\ \frac{e^2}{4\pi\epsilon_0}\ K_0(bq)$, where E_1 is the exponential integral and K_0 the modified Bessel function of 2nd kind.

The static structure factor is defined through the fluctuation-dissipation theorem as

$$S(q) = -\frac{1}{\pi\ n} \int_0^\infty d\omega\ \chi^{''}(q, \omega), \tag{2}$$

where $\chi^{''}(q, \omega)$ is the imaginary part of the density response function (1). The integral in (2) can be re-written using the contour integration method [1] as,

$$S(q) = -\frac{1}{\pi\ n} \int_0^\infty d\omega\ \chi(q, i\omega), \tag{3}$$

where $n = (k_F\ g_s)/\pi$ is the linear electron number density, g_s is the spin degeneracy factor and k_F is the Fermi wave vector. Using the high-density expansion

$$\chi(q, i\omega) = \chi_0(q, i\omega) + \chi_0(q, i\omega)\ V(q)\ \chi_0(q, i\omega), \tag{4}$$

where,

$$\chi_0(q, i\omega) = \frac{g_s m}{2\pi q} \ln\left[\frac{\omega^2 + (\frac{q^2}{2m} - \frac{qk_F}{m})^2}{\omega^2 + (\frac{q^2}{2m} + \frac{qk_F}{m})^2}\right], \tag{5}$$

the structure factor (3) can be calculated for $r_s \to 0$ using (4) and (5) The zeroth-order static structure factor is easily calculated

$$\begin{aligned} S_0(q) &= -\frac{1}{n\ \pi} \int_0^\infty \chi_0(q, i\ \omega) d\omega \\ &= \begin{cases} \frac{q}{2k_F}, & q < 2k_F \\ 1, & q > 2k_F \end{cases}. \end{aligned} \tag{6}$$

The first-order correction to the structure factor can be obtained by substituting $\chi_0(q, i\omega)$ in the second term of (4), and than using it in (3) The resulting integral can be performed analytically and the result for $q < 2k_F$ reads

$$\begin{aligned} S_1(q) = -v(q)\frac{g_s^2\ r_s\ 2k_F}{\pi^2\ q} \Bigg[&\left(1 - \frac{q}{2k_F}\right) \ln\left(1 - \frac{q}{2k_F}\right) \\ &+ \left(1 + \frac{q}{2k_F}\right) \ln\left(1 + \frac{q}{2k_F}\right)\Bigg]. \end{aligned} \tag{7}$$

Similarly, for $q > 2k_F$ one obtains

$$\begin{aligned} S_1(q) = -v(q)\frac{g_s^2\ r_s\ 2k_F}{\pi^2\ q} \Bigg[&\left(\frac{q}{2k_F} - 1\right) \ln\left(\frac{q}{2k_F} - 1\right) \\ &+ \left(1 + \frac{q}{2k_F}\right) \ln\left(1 + \frac{q}{2k_F}\right) - \frac{q}{k_F} \ln\frac{q}{2k_F}\Bigg]. \end{aligned} \tag{8}$$

Here and in the following we use $V(q) = v(q)e^2/4\pi\epsilon_0$. In the limit of small q, q around $2k_F$ and large q, the $S_1(q)$ takes the simpler forms

$$S_1(q) = \begin{cases} -v(q \to 0)\frac{g_s^2\ r_s}{2\pi^2}\frac{q}{k_F}, & q \ll 2k_F \\ -v(q \to 2k_F)\frac{g_s^2\ r_s}{2\pi^2}\frac{k_F}{q}\Lambda(z), & q \to 2k_F \\ -v(q \to \infty)\frac{4g_s^2\ r_s}{\pi^2}\frac{k_F^2}{q^2}, & q \gg 2k_F \end{cases}, \tag{9}$$

where $\Lambda(z) = (8\ln(2) - 2|z| + 2|z|\ln|z| - \frac{3}{4}|z|^2)$ and $z = \frac{q-2k_F}{k_F}$. It can be easily seen that for harmonic wires the interaction potential approaches

$$v(q) = \begin{cases} -\gamma - 2\ln(bq) & \text{for} \quad bq \to 0 \\ 1/(bq)^2 & \text{for} \quad bq \to \infty \end{cases}, \tag{10}$$

with the Euler Gamma constant γ.

For a cylindrical potential the corresponding results are,

$$v(q) = \begin{cases} -\gamma + \ln(2) - \ln(bq) & \text{for} \quad bq \to 0 \\ e^{-bq}\sqrt{\frac{\pi}{2bq}} & \text{for} \quad bq \to \infty \end{cases}. \quad (11)$$

Both potentials behave similarly at the small bq limit, but at large bq they differ. Substituting values of $v(q)$ from (10) in (9), the corresponding leading term agrees with Fogler [20].

To see the effect of thickness b of the wire we calculate the structure factor from (3) by using (1) and (5), for $r_s < 1$ and plot them in Figure 1. It is seen from Figure 1a that as b decreases, the structure factor $S(q)$ also decreases. A similar trend is also obtained for other r_s. To see the validity of the first-order structure factor we plot in Figure 1b for $r_s = 0.1$, $S_0(q) + S_1(q)$ and RPA for $b = 0.025$. These are compared with diffusion quantum Monte Carlo simulation [43] for an infinitely thin wire, as implemented in CASINO code [44]. All three curves match perfectly. It is noted that in the high density limit ($r_s \ll 1$), the structure factor is more or less the one of a non-interacting gas of electrons. This is due to the fact that in this region, the kinetic energy is the dominant contribution to the total energy leading the system to behave as a gas of non-interacting electrons as conjectured by Fogler [20].

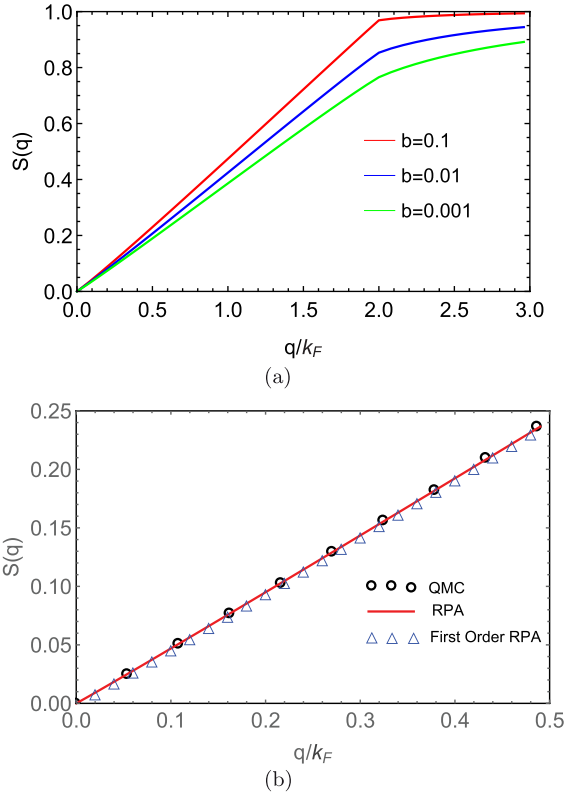

Fig. 1. (a) The static structure factor $S(q)$ in RPA for a cylindrical wire is plotted as a function of q/k_F for $r_s = 0.3$, at different thickness of the wire $b = 0.1$, 0.01 and 0.001 a.u. (b) The RPA structure factor is compared with diffusion Monte Carlo simulation, and with the first order RPA structure factor for $r_s = 0.1$ and $b = 0.025$.

3 Ground state energy

The ground-state energy can be obtained by the density-density response function in conjunction with the fluctuation-dissipation theorem as [1],

$$E_g = E_0 + \frac{n}{2}\sum_{q\neq 0} v(q) \times \left(-\frac{1}{n\pi}\int_0^1 d\lambda \int_0^\infty \chi(q, i\omega; \lambda)\, d\omega\right). \quad (12)$$

It further simplifies into a sum of kinetic energy of the non-interacting gas with the exchange energy and the residual energy (i.e. correlation energy) as,

$$E_g = E_0 + E_x + E_c, \quad (13)$$

where

$$E_x = \frac{n}{2}\sum_{q\neq 0} v(q) \times \left(-\frac{1}{n\pi}\int_0^1 d\lambda \int_0^\infty \chi_0(q, i\omega)\, d\omega - 1\right), \quad (14)$$

$$E_c = \frac{n}{2}\sum_{q\neq 0}\left(-\frac{1}{n\pi}\int_0^1 d\lambda \times \int_0^\infty \frac{\lambda\, v(q)^2\, \chi_0^2(q, i\omega)}{1 - \lambda\, v(q)\, \chi_0(q, i\omega)} d\omega\right). \quad (15)$$

3.1 Exchange energy

In this section the exchange energy for a cylindrical as well as for a harmonic electron wire is obtained analytically, by integrating (14). Specifically for cylindrical wire it turns out to be,

$$E_x = -\frac{Nk_F}{\pi}\left(\frac{2k_F b\, K_1[2k_F b] - 1}{2(k_F b)^2} + \pi K_0[2k_F b] L_{-1}[2k_F b] + \pi K_1[2k_F b]\; L_0[2k_F b]\right), \quad (16)$$

where $K_n(x)$ is nth order modified Bessel function of 2nd kind, and $L_n(x)$ is modified Struve function [45]. Similarly, the exchange energy can also be obtained for a harmonic wire of finite thickness given as

$$E_x = -\frac{Nk_F}{2\pi}\left(G^{2,2}_{2,3}\left(4b^2k_F^2\Big|\begin{matrix}0, \frac{1}{2}\\ 0, 0, -\frac{1}{2}\end{matrix}\right) - \frac{\ln\left(4b^2k_F^2\right) + e^{4b^2k_F^2}\Gamma\left(0, 4b^2k_F^2\right) + \gamma}{4b^2k_F^2}\right), \quad (17)$$

Table 1. Parameters obtained in fitting correlation energy data with the formula given in (30) and (31) for various r_s.

r_s	ϵ	$\alpha_1/\alpha_2/\alpha$	$\beta_1/\beta_2/\beta$	$\eta_1/\eta_2/\eta$	χ^2	ARS	AIC	BIC	RSq	Fig.
0.1	ϵ_{c1}	−0.500	−5.0	−9.15692	–	–	–	–	–	2a
	ϵ_{c2}	0.52184	14.9682	54.0315	0.997365	0.998632	291.265	298.579	0.998721	2a
	ϵ_c	−0.000845452	0.319619	1.31095	1	0.999768	−279.783	−272.469	0.999784	2b
0.01	ϵ_c	−0.000378126	−0.032961	−0.119755	1	0.999925	−544.096	−536.781	0.99993	2c
0.001	ϵ_c	−0.0000108161	−0.00244274	−0.0110844	0.937348	0.99788	−333.214	-329.035	0.998183	2d

where $G^{2,2}_{2,3}\left(4b^2k_F^2|\begin{matrix}0,\frac{1}{2}\\0,0,-\frac{1}{2}\end{matrix}\right)$ and $\Gamma\left(0,4b^2k_F^2\right)$ are the Meijer G function [46] and the incomplete gamma function, respectively. As it is difficult to visualize the former function, it is desirable to write it in its integral form

$$G^{2,2}_{2,3}\left(4r^2|\begin{matrix}0,\frac{1}{2}\\0,0,-\frac{1}{2}\end{matrix}\right) = \int_0^2\left(1-\frac{x}{2}\right)e^{r^2x^2}E_1\left(r^2x^2\right)dx + \frac{\log\left(4r^2\right)+e^{4r^2}\Gamma\left(0,4r^2\right)+\gamma}{4r^2}. \tag{18}$$

For thin harmonic wires $b \ll a_B$ the exchange energy can be simplified to be,

$$E_x = -\frac{Nk_F}{2\pi}(-1-\gamma-\ln(4)-2\ln(k_Fb) -2\,\psi^{(0)}(1/2)+2\,\psi^{(0)}(3/2)), \tag{19}$$

where $\psi^{(0)}(1/2)$ and $\psi^{(0)}(3/2)$ are polygamma functions [45]. We now use the simpler expansion of the polygamma function as $2\,\psi^{(0)}(1/2) = -2\gamma - 2\ln(4)$ and $2\,\psi^{(0)}(3/2) = 4-2\gamma-2\ln(4)$ in the above equation. Equations (16) and (17) can also be written for a polarized gas by defining $k_{F_{\uparrow(\downarrow)}} = k_F(1\pm p)$, $N_{\uparrow(\downarrow)} = N(1\pm p)/2$ and $k_F = \pi/(2g_sr_sa_B)$. Explicitly for thin cylindrical wires $b \ll a_B$, the exchange energy per particle can be obtained by expanding equation (16) as

$$\epsilon_x = -\frac{1}{4g_sr_s}\left((1+p)^2\left[\frac{3}{2}-\gamma-\ln\left(\frac{\pi(1+p)}{2g_sr_s}\right)+\mathcal{L}\right] +(1-p)^2\left[\frac{3}{2}-\gamma-\ln\left(\frac{\pi(1-p)}{2g_sr_s}\right)+\mathcal{L}\right]\right). \tag{20}$$

Similarly for harmonic wires, equation (19) gives

$$\epsilon_x = -\frac{1}{4g_sr_s}\left((1+p)^2\left[\frac{3}{2}-\frac{\gamma}{2}-\ln(2) -\ln\left(\frac{\pi(1+p)}{2g_sr_s}\right)+\mathcal{L}\right]+(1-p)^2\left[\frac{3}{2}-\frac{\gamma}{2} -\ln(2)-\ln\left(\frac{\pi(1-p)}{2g_sr_s}\right)+\mathcal{L}\right]\right), \tag{21}$$

where $\mathcal{L} = \ln(a_B/b)$. It is noted that equations (16) and (17) are new results and for special cases they reduce to (20) and (21). It is worth mentioning that the logarithmic thickness of the wire is defined by $\mathcal{L}^{-1}$. For polarized ($g_s = 1$ and $p = 1$) and unpolarized fluids ($g_s = 2$ and $p = 0$), the exchange energy of a cylindrical wire is obtained respectively to be

$$\epsilon_x = -\frac{\ln(r_s)}{r_s} - \frac{1}{r_s}\left[\frac{3}{2}-\gamma-\ln(\pi)+\mathcal{L}\right], \tag{22}$$

and

$$\epsilon_x = -\frac{\ln(4r_s)}{4r_s} - \frac{1}{4r_s}\left[\frac{3}{2}-\gamma-\ln(\pi)+\mathcal{L}\right]. \tag{23}$$

These are in agreement with Fogler's results [19].

3.2 Correlation energy

The integration over the coupling constant λ is easily done in (15) and the correlation energy becomes

$$E_c = \frac{n}{2}\sum_{q\neq 0}\left(\frac{1}{n\pi}\int_0^\infty\{v(q)\,\chi_0(q,i\omega) +\ln[1-v(q)\,\chi_0(q,i\omega)]\}d\omega\right). \tag{24}$$

The above equation can be written further as,

$$\epsilon_c = \epsilon_{c1}+\epsilon_{c2}, \tag{25}$$

where

$$\epsilon_{c1} = -\frac{g_s}{2\pi}\int_0^\infty v(q)\,S_0(q)\,dq, \tag{26}$$

$$\epsilon_{c2} = \frac{g_s}{2\pi}\int_0^\infty\left(\frac{1}{n\pi}\int_0^\infty\ln\{1-v(q)\,\chi_0(q,i\omega)\}\,d\omega\right)dq. \tag{27}$$

The first term ϵ_{c1} can be integrated analytically for the cylindrical potential,

$$\epsilon_{c1} = -\frac{g_s^2r_sa_B^2}{b^2\pi^2}+\frac{g_sa_B}{b\pi}K_1\left(\frac{b}{a_B}\frac{\pi}{g_sr_s}\right)+\frac{a_B}{2br_s} \times\left[-g_sr_s+\pi(b/a_B)L_{-1}\left(\frac{b}{a_B}\frac{\pi}{g_sr_s}\right)K_0\left(\frac{b}{a_B}\frac{\pi}{g_sr_s}\right)\right] +\left[\pi bL_0\left(\frac{b}{a_B}\frac{\pi}{g_sr_s}\right)K_1\left(\frac{b}{a_B}\frac{\pi}{g_sr_s}\right)\right]. \tag{28}$$

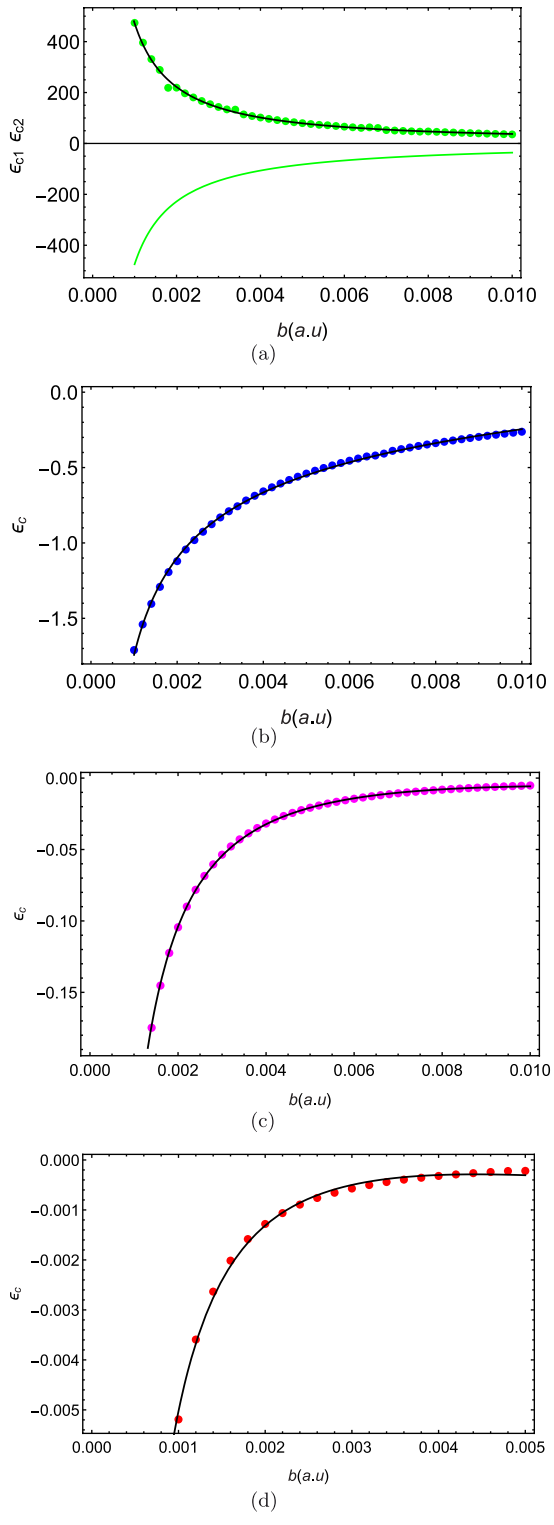

Fig. 2. (a) The parts of correlation energy ϵ_{c1} (lower curve) and ϵ_{c2} (upper curve) versus b for $r_s = 0.1$ where the analytical result ϵ_{c1} (green continuous line) are plotted together with the numerical ϵ_{c2} (green dots) and the fitted curve (black continuous line) for the same r_s. (b) Total correlation energy ϵ_c for the same value of r_s with the fitted curve (black continuous line) and the numerical results (blue dots). (c) and (d) for $r_s = 0.01$ and $r_s = 0.001$ respectively, but numerical results (dots) are shown by magenta and red colors.

Equation (28) is further simplified for an infinitely thin wire $b \to 0$ for any finite r_s as

$$\epsilon_{c1} = \frac{-g_s}{2(b/a_B)} + \frac{1}{2r_s}\left[\frac{3}{2} - \gamma + \ln\left(\frac{a_B}{b}\right) - \ln\left(\frac{\pi}{2g_s r_s}\right)\right]. \quad (29)$$

For a given r_s the above equation has a functional dependence on b (in atomic unit) as

$$\epsilon_{c1}(b, r_s) = \frac{\alpha_1(r_s)}{b} + \beta_1(r_s)\ \ln(b) + \eta_1(r_s), \quad (30)$$

where $\alpha_1(r_s)$, $\beta_1(r_s)$ and $\eta_1(r_s)$ can be read from (29). Equation (27) cannot be integrated analytically, therefore we solve it numerically. Anticipating that the correlation energy ϵ_c for $b \to 0$ and $r_s \to 0$ turns out to be a constant, ϵ_{c2} may also be represented by (30) but with the coefficients $\alpha_2(r_s)$, $\beta_2(r_s)$ and $\eta_2(r_s)$. Therefore we represent ϵ_{c2} by,

$$\epsilon_{c2}(b, r_s) = \frac{\alpha_2(r_s)}{b} + \beta_2(r_s)\ \ln(b) + \eta_2(r_s), \quad (31)$$

and fit it to the numerical result. The coefficients α, β, η for ϵ_{c2} and ϵ_c are given in Table 1, for r_s=0.1, 0.01 and 0.001. Note that the coefficients for ϵ_{c1} are analytically known. Also the same formula as for ϵ_{c2} is assumed for ϵ_c. To estimates the accuracy of the fit with the numerical calculation, we have provided the statistical analysis with different methods: χ^2, R^2 adjusted for the number of model parameters, AdjustedRSquared (ARS), Akaike information criterion (AIC), Bayesian information criterion (BIC) and coefficient of determination R^2 (RSq). The fitted parameters by the statistical analysis in Table 1 reflect the quality of the function $\epsilon_{c2}(b, r_s)$ and $\epsilon_c(b, r_s)$.

The correlation energies per particle ϵ_{c1} (lower curve) and ϵ_{c2} (upper curve) are plotted in Figure 2a, as obtained analytically and numerically, and are shown as green continuous curve and green dots, respectively. The fitted ϵ_{c2} from representation (31) is shown by the black continuous line. It is clearly seen that there is a perfect fit of ϵ_{c2}, as also inferred above from the statistical analysis. It is seen that there is no cancellation between the two curves for $r_s = 0.1$. The resulting sum is plotted for the same r_s in Figure 2b. Total correlation energy for $r_s = 0.01$ and $r_s = 0.001$ are also plotted in Figures 2c and 2d respectively. These figures show that there is no indication that the correlation energy approaching a constant value for very small r_s for an infinitely thin wire.

For a pragmatic width of the wire, the correlation energy for a polarized fluid is reported in Table 2. The correlation energy at high densities $r_s \leq 0.1$ and $b = 0.1$, is in agreement with the quantum Monte Carlo simulation [36,37] for polarized fluids.

To check the consistency of our result of the correlation energy for $b \to 0$ and $r_s < 1$, we plot it in Figure 3 as a function of r_s for small values of b. It is seen that as b decreases, the correlation energy increases,

Table 2. Correlation energy per particle for fully polarized fluids for various r_s and b.

r_s / b	Correlation energy ϵ_c (mHartree)						
	0.001	0.01	0.1	0.2	0.3	0.4	0.5
0.001	−5.1925	−0.051326	−0.00051321	−0.000128314	−0.000057025	−0.00032081	−0.000205298
0.01	−267.9063	−5.18143	−0.0512140	−0.01280232	−0.00568998	−0.00320059	−0.002048385
0.1	−1675.0533	−258.96748	−5.075932	−1.2577678	−0.5580828	−0.3137399	−0.20074031
0.2	−2250.7232	−568.01835	−19.866556	−4.9634643	−2.1935919	−1.2308436	−0.7868883
0.3	−2543.4151	−684.53832	−41.492422	−11.018708	−4.8636832	−2.7297174	−1.7380320
0.4	−2714.8034	−814.49113	−66.343762	−19.104517	−8.5835144	−4.7704732	−3.0480646
0.5	−2815.2034	−895.4	−93.330872	−28.570889	−13.510079	−7.3493536	−4.6830739

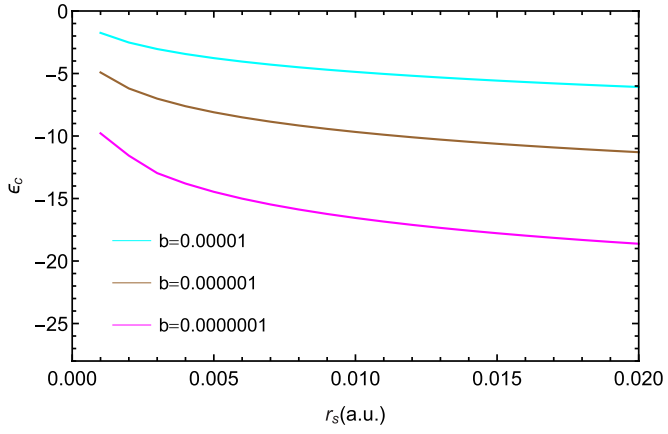

Fig. 3. The correlation energy per particle versus r_s for different thicknesses b of a cylindrical wire.

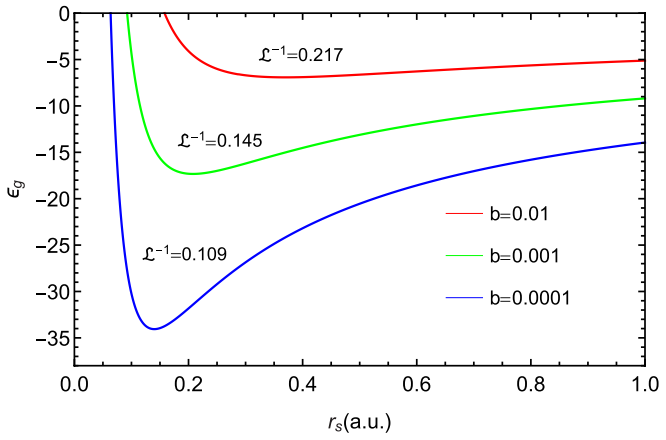

Fig. 4. Ground state energy ϵ_g is plotted as a function of $r_s \leq 1$, for values of wire widths b.

which is consistent with our previous results given in Figures 2b–2d.

In Figure 4 the total ground-state energy is presented with different wire thicknesses as a function of r_s. As b decreases, the ground-state energy increases. For the range $r_s \ll 1$ there are no QMC data available to compare the ground-state energy for an infinitely thin wire. Our calculation is suited for long-range interactions whereas the Fogler calculation deals with the short-range interaction.

4 Summary

In this paper we have calculated the dependence of the ground-state structure factor and the correlation energy on the thickness of an electron wire as a function of r_s. The structure factor is calculated in the single-loop approximation of RPA. The electron-electron interactions are modeled by a cylindrical and a harmonic potential. We find an agreement with the variational calculation of Fogler [20]. The structure factor has also been compared for $b = 0.025$ and $r_s = 0.1$ with the QMC data [43]. For first-order corrections in the interaction, the RPA results and the QMC data match perfectly, indicating that for small thickness and for high densities, the electron gas behaves as a gas of non-interacting particles though highly correlated, which is clear from the correlation energy calculations. In this sense Fogler [19,20] calls it a Coulomb-Tonks gas.

We have also obtained new analytical expressions for the exchange energy of both cylindrical and harmonic electron wires. In the small-thickness limit the expressions simplify considerably and are more or less the same for both wires. This has been also worked out for polarized gases, from which the paramagnetic and ferromagnetic phases can easily be obtained. The exchange energy for a fully polarized gas agrees with Fogler [19].

In the present paper the total correlation energy in RPA is found to be fitted by

$$\epsilon_c(b, r_s) = \frac{\alpha(r_s)}{b} + \beta(r_s)\ \ln(b) + \eta(r_s), \qquad (32)$$

with the parameters given explicitly. This correlation energy is the sum of two terms which only partially cancel. The first term is calculated analytically exactly by the expression (32) where the values of α, β and η are precisely known. The second term has been calculated numerically. It perfectly fits with the expression of (32) but with different parameters.

This findings clearly indicate that the correlation energy is diverging in the limit of $b \to 0$ and $r_s \to 0$. Further, the correlation energy as a function of r_s for various b, again points out that the correlation energy increases as b decreases for $r_s \to 0$. The Coulomb correlations are enhanced, and the interacting electron gas behaves structure-less in the ultra-thin and high-density domain of $\mathcal{L}^{-1} \ll r_s \ll 1$ like a strongly-interacting electron gas

named Coulomb-Tonks gas [19,20]. Further, we find that the correlation energy does not approach a constant value for an infinitely thin wire and $r_s \to 0$ within the RPA.

The authors (VA and KNP) acknowledge the financial support by National Academy of Sciences of India. KM like to thank for the support of the visit to Panjab university by Indian National Science Academy and DFG. The high performance computing centre facilities at Panjab University has been used to run the CASINO code for quantum Monte Carlo calculations. Open access funding provided by Max Planck Society.

Author contribution statement

All the authors were involved in the preparation of the manuscript. All the authors have read and approved the final manuscript.

References

1. G.F. Giuliani, G. Vignale, *Quantum theory of the electron liquid* (Cambridge University Press, Cambridge, 2005)
2. R. Saito, G. Dresselhaus, M.S. Dresselhaus, *Physical properties of carbon nanotubes* (Imperial College Press, London, 1998)
3. M. Bockrath, D.H. Cobden, J. Lu, A.G. Rinzler, R.E. Smalley, L. Balents, P.L. McEuen, Nature **397**, 598 (1999)
4. H. Ishii, H. Kataura, H. Shiozawa, H. Yoshioka, H. Otsubo, Y. Takayama, T. Miyahara, S. Suzuki, Y. Achiba, M. Nakatake, T. Narimura, M. Higashiguchi, K. Shimada, H. Namatame, M. Taniguchi, Nature **426**, 540 (2003)
5. M. Shiraishi, M. Ata, Solid State Commun. **127**, 215 (2003)
6. J. Schäfer, C. Blumenstein, S. Meyer, M. Wisniewski, R. Claessen, Phys. Rev. Lett. **101**, 236802 (2008)
7. Y. Huang, X. Duan, Y. Cui, L.J. Lauhon, K.-H. Kim, C.M. Lieber, Science **294**, 1313 (2001)
8. H. Monien, M. Linn, N. Elstner, Phys. Rev. A **58**, R3395 (1998)
9. A. Recati, P.O. Fedichev, W. Zwerger, P. Zoller, J. Opt. B: Quantum Semiclass. Opt. **5**, S55 (2003)
10. H. Moritz, T. Stoferle, K. Guenter, M. Kohl, T. Esslinger, Phys. Rev. Lett. **94**, 210401 (2005)
11. F.P. Milliken, C.P. Umbach, R.A. Webb, Solid State Commun. **97**, 309 (1996)
12. S.S. Mandal, J.K. Jain, Solid State Commun. **118**, 503 (2001)
13. A.M. Chang, Rev. Mod. Phys. **75**, 1449 (2003)
14. A. Nitzan, M.A. Ratner, Science **300**, 1384 (2003)
15. S. Tomonaga, Prog. Theor. Phys. **5**, 544 (1950)
16. J.M. Luttinger, Phys. J. Math. **4**, 1154 (1963)
17. F.D.M. Haldane, J. Phys. C **14**, 2585 (1981)
18. H.J. Schulz, Phys. Rev. Lett. **71**, 1864 (1993)
19. M.M. Fogler, Phys. Rev. Lett. **94**, 056405 (2005)
20. M.M. Fogler, Phys. Rev. B **71**, 161304(R) (2005)
21. M. Fabrizio, A.O. Gogolin, S. Scheidl, Phys. Rev. Lett. **72**, 2235 (1994)
22. S. Capponi, D. Poilblanc, T. Giamarchi, Phys. Rev. B **61**, 13410 (2000)
23. G. Fano, F. Ortolani, A. Parola, L. Ziosi, Phys. Rev. B **60**, 15654 (1999)
24. D. Poilblanc, S. Yunoki, S. Maekawa, E. Dagotto, Phys. Rev. B **56**, R1645 (1997)
25. B. Valenzuela, S. Fratini, D. Baeriswyl, Phys. Rev. B **68**, 045112 (2003)
26. W.I. Friesen, B. Bergersen, J. Phys. C **13**, 6627 (1980)
27. L. Calmels, A. Gold, Phys. Rev. B **56**, 1762 (1997)
28. V. Garg, R.K. Moudgil, K. Kumar, P.K. Ahluwalia, Phys. Rev. B **78**, 045406 (2008)
29. M. Tas, M. Tomak, Phys. Rev. B **67**, 235314 (2003)
30. R. Bala, R.K Moudgil, S. Srivastava, K.N. Pathak, J. Phys.: Condens. Matter **24**, 245302 (2012)
31. R. Bala, R.K. Moudgil, S. Srivastava, K.N. Pathak, Eur. Phys. J. B **87**, 5 (2014)
32. C.R. de Oliveira, A.A. Verri, Ann. Phys. **324**, 251 (2009)
33. L.O. Wagner, E.M. Stoudenmire, K. Burke, S.R. White, Phys. Chem. Chem. Phys. **14**, 8581 (2012)
34. E.M. Stoudenmire, L.O. Wagner, S.R. White, K. Burke, Phys. Rev. Lett. **109**, 056402 (2012)
35. R.M. Lee, N.D. Drummond, Phys. Rev. B **83**, 245114 (2011)
36. M. Casula, S. Sorella, G. Senatore, Phys. Rev. B **74**, 245427 (2006)
37. A. Malatesta, Quantum Monte Carlo study of a model one-dimensional electron gas, Ph.D. thesis, Universita Degli studi Di Trieste, Departmento di Fisica Teorica, 1999
38. L. Shulenburger, M. Casula, G. Senatore, R.M. Martin, Phys. Rev. B **78**, 165303 (2008)
39. A. Malatesta, G. Senatore, J. Phys. IV **10**, 5 (2000)
40. P.F. Loos, J. Chem. Phys. **138**, 064108 (2013)
41. K. Morawetz, V. Ashokan, R. Bala, K.N. Pathak, to be published
42. D. Pines, P. Nozieres, *The theory of quantum liquids* (W.A. Benjamin, Inc., New York, 1966)
43. V. Ashokan, N.D. Drummond, K.N. Pathak, to be published
44. R.J. Needs, M.D. Towler, N.D. Drummond, P.L. Ríos, J. Phys.: Condens. Matter **22**, 023201 (2010)
45. *Handbook of mathematical functions*, edited by M. Abramowitz, I. Stegun (Dover Publications, Inc., New York, 1972), pp. 498 and 260
46. H. Bateman, A. Erdélyi, *Higher transcendental functions* (McGrawHill, New York, 1953), Vol. I, p. 206 (see 5.3, Definition of the G-Function)